An analysis of ZTEM data over the Mt Milligan Porphyry Copper Deposit, British Columbia

Daniel Sattel, EM Solutions LLC, Scott Thomas, Condor Consulting, Inc. and Michael Becken, GFZ Potsdam*

Summary

ZTEM is a passive helicopter-borne system that measures the magnetic field response in the frequency range 30-720 Hz of naturally occurring currents in the subsurface. The resolution of this system is analyzed by forward modeling and inverting synthetic ZTEM data using a 2D algorithm for a range of conductivity scenarios.

ZTEM data acquired across the Mt Milligan Cu-Au porphyry system are compared with overlapping VTEM data. Conductivity-depth sections derived from both data sets show broad agreement, but indicate better spatial resolution for the VTEM data. Neither data set appears to show a significant response from the Cu-Au mineralization. Products derived from the ZTEM data, including apparent conductivity, phase and Karous-Hjelt filtered grids appear to map geologic structure.

Introduction

The ZTEM system has been available for commercial surveys for only a couple of years and reported case studies are therefore limited (Legault et al., 2009a, 2009b). It measures the magnetic-field response of naturally occurring subsurface currents, induced by far-away lightning discharges. By comparison, the VTEM system measures the magnetic-field response due to currents induced in the subsurface by the transmitter the system is carrying and many case studies have been reported in the literature (e.g. Witherly and Irvine, 2007).

As part of Geoscience BC's QUEST project, both the Geotech VTEM and ZTEM systems have been flown over Mount Milligan, an alkalic Cu-Au porphyry system located in British Columbia, 155 km northwest of Prince George. It should be noted that this type of mineralization is expected to be a difficult target for an electromagnetic system due to generally being associated with relatively low conductivities. However, by being sensitive to conductivity contrasts, the ZTEM system might have an advantage in resistive terrain. The overlap of data from both surveys allow for a direct comparison of the spatial resolution and depth penetration of the two systems.

The survey flight paths overlain on the Mt Milligan geology are shown in Figure 1. The VTEM data were acquired in 2007 at a line spacing of 200 m; the ZTEM survey was flown in 2008 with a line spacing of 250 m.

Before analyzing the survey data, synthetic modelling of the ZTEM data is presented, to illustrate the strengths and limitations of that system.

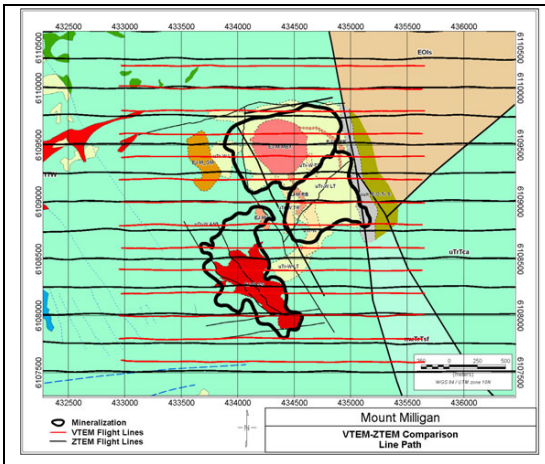

Figure 1: Flight path of VTEM and ZTEM surveys overlain on the geology of the Mt Milligan porphyry system.

Synthetic ZTEM data

Synthetic ZTEM profiles were forward modeled and inverted using a 2D MT algorithm, developed by Constable and Wannamaker (deGroot-Hedlin and Constable, 1990; Wannamaker at al., 1987; deLugao and Wannamaker, 1996). The inversion fitted the data to a RMS error of 1.3, which has been determined as a representative target RMS for the modeling of survey data.

Synthetic modeling results are shown in Figures 2-4. A flying height of 80 m was modeled. The insensitivity of the ZTEM system to one-dimensional or layered conductivity structures is illustrated in Figure 2. Since the vertical magnetic field, due to plane-wave excitation (magnetotelluric Hz response) is zero above a 1D earth, the ZTEM system tipper-functions Tzx and Tzy, that are determined from the magnetic field observations by statistical analysis of the relationship

$$H_z = \begin{bmatrix} T_{zx} & T_{zy} \end{bmatrix} \begin{bmatrix} H_x \\ H_y \end{bmatrix} \quad (1)$$

show no response above a layered-earth. However, the 2D inversion will still derive a resistive half-space since that

model is used to initialize the inversion. In Equation (1), the vertical magnetic field is measured in the air, and the horizontal components are recorded with a fixed ground station.

The sensitivity to two-dimensional conductivity structures is demonstrated with the quarter-space model in Figure 3.

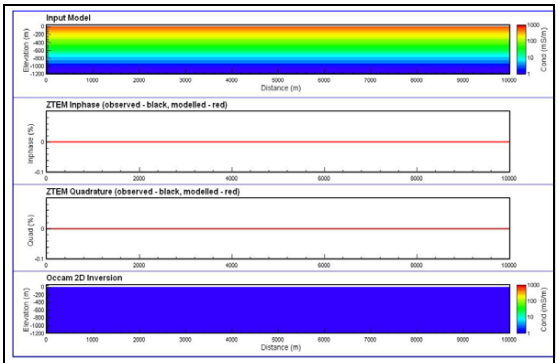

Figure 2: Observed and modelled ZTEM responses above a layered-earth conductivity structure.

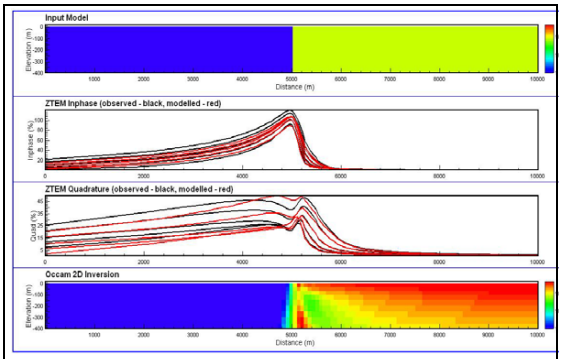

Figure 3: Observed and modelled ZTEM responses across a contact of quarter-spaces.

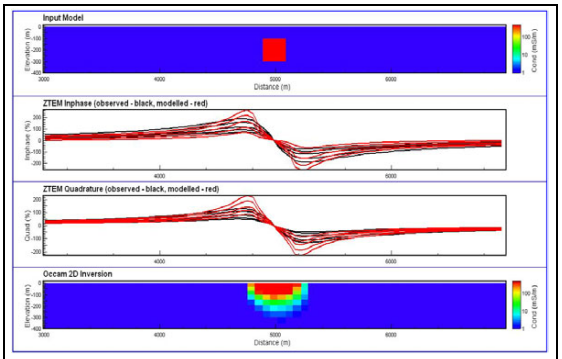

Figure 4: Observed and modelled ZTEM responses above a tabular conductor.

The ZTEM system shows a strong Tzx response at the contact of the two quarter-spaces and the 2D inversion resolves the conductivity contrast well. However, the modeled conductivity structure at the contact could be mistaken for a discrete conductor.

The ZTEM response across a tabular conductor is shown in Figure 4. The ZTEM system shows a strong Tzx response above the conductor and the 2D inversion gives a good indication of the conductor's presence, albeit at a depth range that is shallower than the actual depth of the conductor.

Mt Milligan Survey

Comparison VTEM – ZTEM

A conductivity-depth section derived from VTEM data by layered-earth inversion is shown in Figure 5. The line shown crosses the Cu-Au mineralization, for which there is no indication on the conductivity-depth section.

The derived conductivity-structure of that line was forward modelled to predict the expected ZTEM response using the 2D MT algorithm, taking into account the system elevation. Since the ZTEM line coincident with the VTEM data is longer, the conductivity structure was extrapolated at both ends. A comparison between observed and predicted ZTEM data is shown in Figure 5. There is overall agreement in the profile shape, but some difference in amplitudes. The observed ZTEM quadrature profile displays strong signal modulation most likely caused by bird swing.

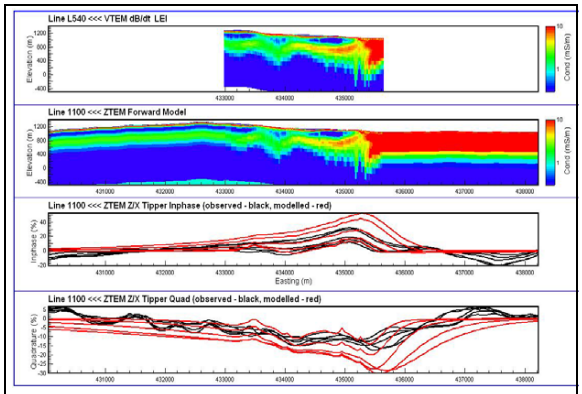

Figure 5: Conductivity-depth section deried from VTEM data (top), extrapolated conductivity-depth section used to predict ZTEM data, observed and predicted ZTEM inphase and quadrature profiles (bottom)

Next, the ZTEM data were modelled using the 2D inversion algorithm by Constable and Wannamaker. The

inversion result of the ZTEM data from Figure 5 is shown in Figure 6.

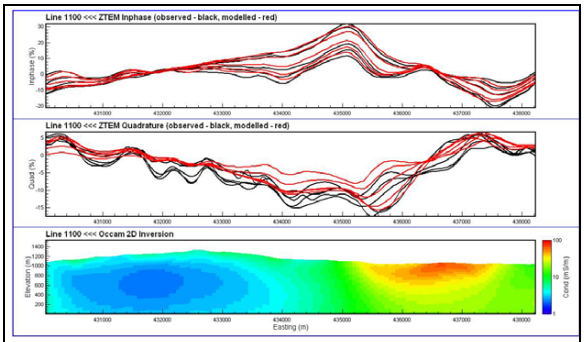

Figure 6: Observed and modelled ZTEM responses with derived conductivity-depth section.

The derived conductivity structure agrees with the VTEM results, ie conductive material is mapped to the east, while the western half is moderately resistive. However, the ZTEM-derived conductivity-depth section lacks spatial resolution compared to the VTEM section.

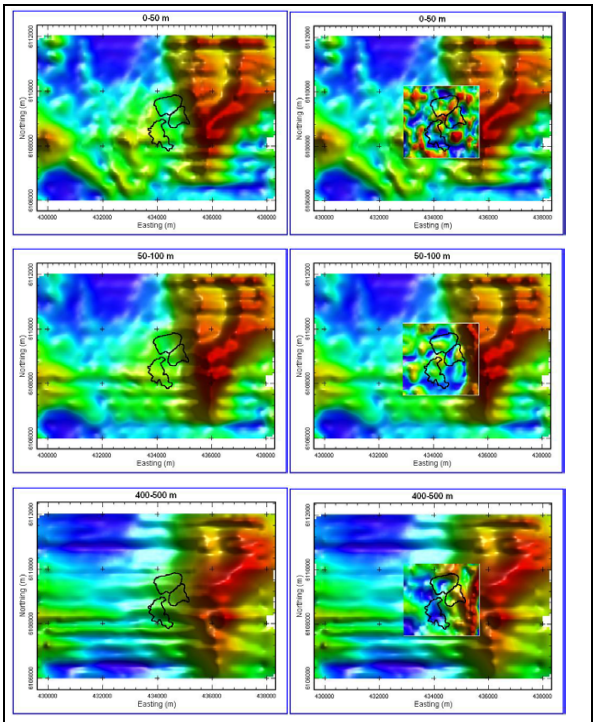

Figure 7: Left panel: conductivity-depth grids derived from ZTEM 2D inversions at depth ranges 0-50 m, 50-100 m and 400-500 m (top to bottom). Right panel: same as left panel with VTEM conductivity-grids overlain on ZTEM grids. Known mineralizations are outlined in black. The resistors seen in the VTEM are the resistive stocks.

Conductivity-depth grids have been derived from the conductivity-depth sections of all ZTEM lines. Figure 7 shows the conductivity at shallow and intermediate depths. Conductivity-depth grids derived from VTEM inversions are inserted on the spatially more extensive ZTEM grids. The two data sets agree on mapping the western edge of the conductive unit associated with the Great Eastern Fault Zone.

Karous-Hjelt Filter

Pseudo-sections derived with the Karous-Hjelt filter (Karous and Hjelt, 1983) can be useful to extract subtle conductors from the ZTEM profiles. The main property of the Karous-Hjelt filter is to turn cross-overs into peaks. Figure 8 shows pseudo-sections derived from the inphase profile of each frequency. Even though the derivation of Karous-Hjelt sections is far less sophisticated than running 2D inversions, these sections agree overall with the 2D inversion result, mapping near-surface conductors to the east and resistive material to the west.

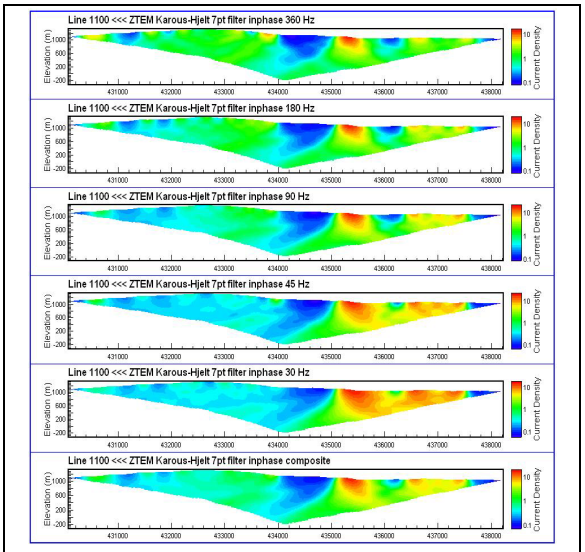

Figure 8: Karous-Hjelt sections derived from inphase ZTEM profiles with decreasing frequency from top to bottom and a composite section of all frequencies at the very bottom.

Near-surface grids of the Karous-Hjelt filtered ZTEM data are shown in Figure 9. These grids are similar to divergence grids generated by Geotech that are based on the VLF peaker derivation (Pedersen et al., 1994). The latter however makes use of the spatial derivatives of the Tzx and Tzy Tippers, whereas the Karous-Hjelt filter is derived only from the Tzx Tipper data. These grids indicate geologic structures striking NNW-SSE, including the Great Eastern Fault Zone.

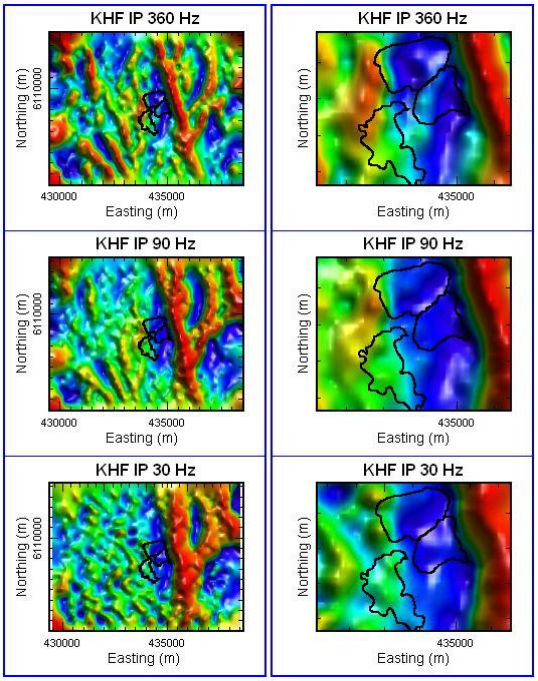

Figure 9: Karous-Hjelt near-surface grids. The entire survey is shown in the left panels, a close-up in the right panels, with known mineralizations outlined in black.

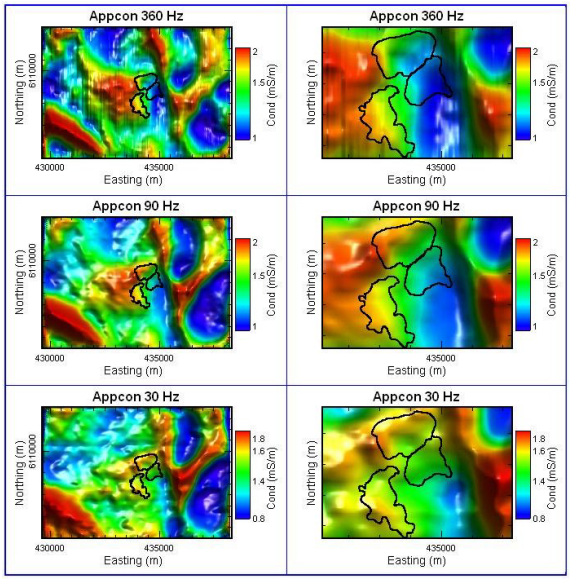

Figure 10: Apparent conductivities derived jointly from ZTEM Tzx and Tzy responses 30-360 Hz. The entire survey is shown in the left panels, a close-up in the right panels, with known mineralizations outlined in black.

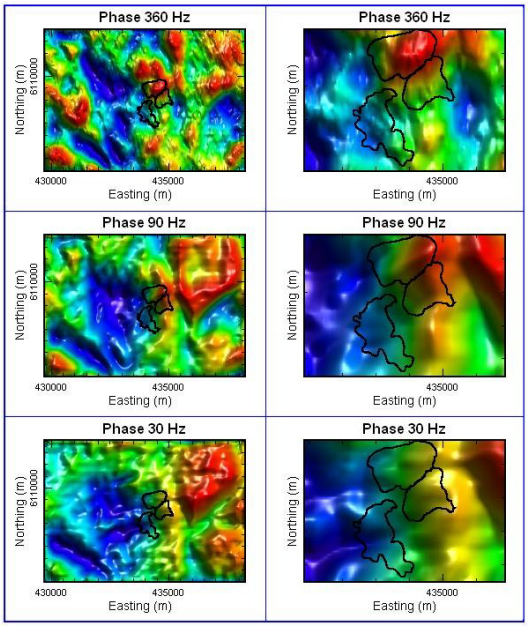

Figure 11: Phases derived jointly from ZTEM Tzx and Tzy responses 30-360 Hz.

Apparent Conductivity and Phase

The derivation of apparent conductivity and phase from VLF data is discussed by Becken and Pedersen (2003). The method has been applied to the Mt Milligan ZTEM data, making joint use of the Tzx and Tzy tippers. The derived apparent conductivities and phases are shown in Figures 10 and 11. These images indicate geological structures, such as the Great Eastern Fault Zone, and a conductive zone west of the known mineralization.

Conclusions

The analysis of VTEM and ZTEM data at Mt Milligan has indicated that conductivity-sections and conductivity-depth grids derived from ZTEM data via 2D inversion show less spatial resolution than corresponding VTEM products. However, some of the products derived from ZTEM data, including apparent conductivity grids, complement the information gained from a VTEM survey.

Although the resistive stock is discernable, the ZTEM data and derived products do not appear to indicate the known mineralization at the Mt Milligan porphyry copper deposit, a difficult exploration target for electromagnetic surveys due to its expected low conductivity.

EDITED REFERENCES

Note: This reference list is a copy-edited version of the reference list submitted by the author. Reference lists for the 2010 SEG Technical Program Expanded Abstracts have been copy edited so that references provided with the online metadata for each paper will achieve a high degree of linking to cited sources that appear on the Web.

REFERENCES

Becken, M., and L. B. Pedersen, 2003, Transformation of VLF anomaly maps into apparent resistivity and phase: Geophysics, **68**, 497–505, doi:10.1190/1.1567218.

DeGroot-Hedlin, C., and S. Constable, 1990, Occam's inversion to generate smooth two-dimensional models from magnetotelluric data: Geophysics, **55**, 1613–1624, doi:10.1190/1.1442813.

De Lugao, P. P., and P. Wannamaker, 1996, Calculating the two-dimensional magnetotelluric Jacobian in finite elements using reciprocity: Geophysical Journal International, **127**, no. 3, 806–810, doi:10.1111/j.1365-246X.1996.tb04060.x.

Karous, M., and S. E. Hjelt, 1983, Linear filtering of VLF dip-angle measurements: Geophysical Prospecting, **31**, no. 5, 782–794, doi:10.1111/j.1365-2478.1983.tb01085.x.

Legault, J. M., H. Kumar, B. Milicevic, and P. Wannamaker, 2009, ZTEM tipper AFMAG and 2D inversion results over an unconformity uranium target in northern Saskatchewan: 79th International Exposition and Annual Meeting, SEG, Expanded Abstracts, 1277-1281.

Legault, J. M., H. Kumar, B. Milicevic, and L. Hulbert, 2009, ZTEM airborne tipper AFMAG test survey over a magmatic copper-nickel target at Axis Lake in northern Sakatchewan: 79th International Exposition and Annual Meeting, SEG, Expanded Abstracts, 1272-1276.

Pedersen, L. B., W. Qian, L. Dynesius, and P. Zhang, 1994, An airborne tensor VLF system. From concept to realization: Geophysical Prospecting, **42**, no. 8, 863–883, doi:10.1111/j.1365-2478.1994.tb00246.x.

Wannamaker, P. E., J. A. Stodt, and L. Rijo, 1987, A stable finite-element solution for two-dimensional magnetotelluric modeling: Geophysical Journal of the Royal Astronomical Society, **88**, 277–296.

Witherly, K., and R. Irvine, 2007, Mapping targets of high conductance with the VTEM airborne EM system: 19th International Geophysical Conference and Exhibition, ASEG, Extended Abstracts.